ANALYSIS OF WRIST EXTENSION USING DIGITAL IMAGE CORRELATION

S.N. Omkar[1] and Amarjot Singh[2]
[1]*Department of Aerospace Engineering, Indian Institute of Science, Bangalore, India*
E-mail: omkar@aero.iisc.ernet.in
[2]*Department of Electrical and Electronics Engineering, National Institute of Technology Warangal, India*
E-mail: amarjotsingh@ieee.org

Abstract

Carpal Tunnel Syndrome also known as median neuropathy is a painful disorder of the wrist and hand. It is a medical condition arising due to the abbreviation of the median nerve in the vicinity of carpal tunnel, resulting in numbness, parenthesis and muscle weakness in hand. We present an effective optical approach for the measurement of strain on superficial muscles and tendons due to wrist extension, a remedy for carpal tunnel syndrome. The DIC code developed computes the in-plane strain with a correlation function using pictures taken, using a CCD camera, before and after extension. The shift between the initial picture and subsequent one is performed by computation of cross-correlation using FFT. This study can assist practitioners working in the field of applied anthropology to develop advanced diagnosis methodologies.

Keywords:

Digital Image Correlation, Carpal Tunnel Syndrome, Wrist Extension

1. INTRODUCTION

Wrist is an extremely significant and important part of our body. It is the performance index of our work. It is determinant for optimal performance of the work carried out by a human being [1]. Disciplines such as ergonomics, anthropology and bio-mechanics deal with various aspects of wrist related postures. These disciplines specifically aim at designing job environment to prevent repetitive strain injuries. A great deal of work has been carried out related to the injuries related to the wrist and work environment [2].

Many wrist related hazards have been associated with the occupation of the patient. The disorders can be directly linked with the working environment of the patient and in addition with the nature of the work [3]. The injuries related to the wrist are classified as repetitive strain injury (RSI) also known as (repetitive motion disorder (RMD), cumulative trauma disorder (TMD), overuse syndrome). This injury is associated with musculoskeletal and nervous systems resulting from repetitive motions, vibrations, compressions etc.

The primary reason associated with these injuries is the repetitive tasks in the working environment [4]. Risk factors are always co relational and may or may not cause an effect. Occupational risk factors associated with the repetitive tasks in the working environment has been cited regularly. Such inhospitable conditions can cause damage to the tendons passing through the wrist leading to swelling and severe pain. One of the major factors linked to injuries is the swelling of the flexor tendons. Median nerve passing through the wrist is compressed across the carpal tunnel due to swelling resulting into carpal tunnel syndrome (CTS).

The remedy of wrist extension relates to Carpal Tunnel Syndrome [5], [6], first quoted in medical literature in 1939 by physician Dr. George S. Phalen [7]. CTS is a grievous disorder resulted by the abbreviation of the median nerve in the vicinity of carpal tunnel. Carpal tunnel dwelling of CTS is enclosed by bones on three sides with a carpal ligament on the fourth side. Carpal tunnel accommodates nine flexor tendons of the hand, passing through the tunnel. The median nerve passing through the carpal tunnel is abbreviated by reduction in the size of the carpal tunnel or with augmentation in the size of tissues (swelling) around flexor tendons or both. The median nerve gets compressed with its movement down to the transverse carpal ligament (TCL) resulting into weakness of the flexor pollicis brevis, opponens pollicis, abductor pollicis brevis, as well as sensory loss in the distribution of the median nerve distal to the transverse carpal ligament.

The most important causes of CTS are related with the biological and structural activities rather than the environmental ones [8]. Study performed by Gross et. al., [9] proved the dominance of force as a major risk factor. However Dr. Peter Nathen stated vibrations as the prime risk factor at the American occupational conference in 1996**.** Genetic predisposition is also considered as a major risk factor. In many parts of the world CTS concludes into multi billion dollars worker compensation claims every year [10].

A number of techniques are being used for the analysis and treatment of CTS. The major remedies include splinting or bracing, steroid injection, activity modification, physical or occupational therapy (controversial), medications, and surgical release of the transverse carpal ligament are often used to cure the syndrome. Recent developments in ergonomics have lead to changes in working environment in the industries. A number of ergonomic measures have been aimed at preventing CTS. In order to apply the remedies discussed above, it is essential to analyze CTS before. Since the effects of all the factors can be studied by the variations in wrist postures (both wrist extension and wrist flexion), the author aims to come up with a method to analyze the strain field on the superficial muscles and tendons of the top surface of fore arm without any dependence of specialist. The author aims at using digital imaging to analyze and assist diagnosis for wrist extension.

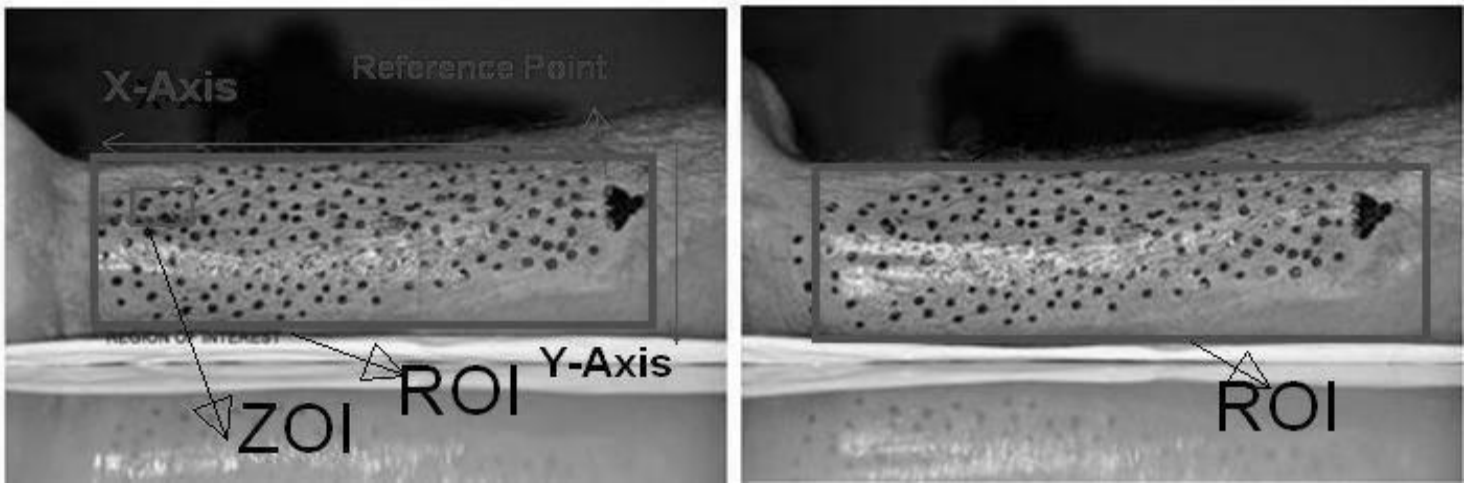

(a) (b)

Fig.1. Wrist Extension Experiment: (a) Reference Image (b) Deformed Image

Digital Imagery has being used over a number of years to compute and evaluate strain for a number of applications. 1-d time delay estimation techniques were used initially for displacement and strain estimation [11] while the evaluation of 2-d strain has been developed, using both B-mode data [12] and raw radio frequency (rF) data [13]. These strain-imaging techniques are put into practice mainly for cardiovascular applications [14] and breast and prostate tumor research [15]. A number of groups have been exploring the opportunity of shear strain imaging and its possible applications [16]. In addition, shear strain imaging has been of active attraction for classification of breast tumors [17] and cardiovascular applications [18]. Rotation and, especially, torsion are vastly studied in cardiovascular research [19]. Apart from the biomedical application, digital imaging has made its mark in a number of other applications including the measurement of deformation and strain in rail vehicle safety [20], air-plane safety [21] etc. The methodology is also implemented for evaluation of in-plane deformation characteristics of geo-materials [22], and to evaluate local failure of bone, in medical field [23].

In the past, the measurement of strain was restricted to a specified location in a structure i.e. it was impossible to compute the strain distribution over the whole structure. A number of false attempts were made to evaluate strain values at large number of locations by making use of discrete targets due to the computational power requirements. A few techniques such as Moiré Interferometry [24], holographic Interferometry [25], speckle photography [26] have been proposed to acquire the overall deformation contour, but it is often time consuming and involves heavy computational power. On the other hand, Digital Image Correlation (DIC) is a simple and quick state-of-art technique superior to previous techniques due to its ability to compute faster.

DIC was first developed by researchers from the University of South Carolina [28]. The concept behind the method was to compute the displacement of the material under test by tracking the deformation of speckle pattern from using digital photography performed during the experiment [27]. DIC method is famous for its simplicity and easy processing. In addition, it is a technique with non–contact, non destructive and full field measurement capability. A large number of algorithms [30] have been developed over the years in order to find the solutions through DIC. Among these methods, the most commonly used algorithm involves an iterative solution that computes the maximum value of cross-correlation coefficient lying in the parameter space [38]. A correlation function is used to compute the shift between the two images. The algorithm is highly effective when precise displacement between two images have to be calculated. Digital Image correlation has proven to be an extremely effective optical approach with vast applications like evaluating properties of human soft tissue in vivo [31], direct computation of two-dimensional strain distributions in interior of articular cartilage under unconfined compression [32], measuring Osteocyte lacunae tissue strain in cortical bone [33], determining local mechanical conditions within early bone callus [34] etc. DIC has been used to study the stress patterns in solder interconnects of BGA packages under thermal loading [35], [36] material characterization under thermal loading [37], dynamic testing to study deformation for flexible bodies [39], material classification at high strain rate [40], stresses and strain in flip-chip die under thermal loading [41] etc.

DIC has been applied multiple times in the past in the field of applied anthropology to assist practitioners for diagnosis [46]. DIC has been made into practice used to study the mechanical properties of biological soft tissues e.g. using 2D DIC: on the human tympanic membrane [42], sheep bone callus [34], human cervical tissue [43] and recently also using 3D DIC: for the bovine cornea [44] and mouse arterial tissue [45]. A number of algorithms have been developed and applied to evaluate the strain pattern due to the force applied on different body parts. A correlation function can be used to evaluate the shift between the two images taken before and after the deformation by tracking the speckle pattern, leading to evaluation of strain. The evaluation of cross-correlation can be performed in the physical space [47] or in the Fourier space using Fast Fourier Transform (FFT) [48]. The intermediate cross correlation FFT step can involve heavy computations depending upon the field due to the heavy computational complexity of the speckle pattern [49], [50], [51].

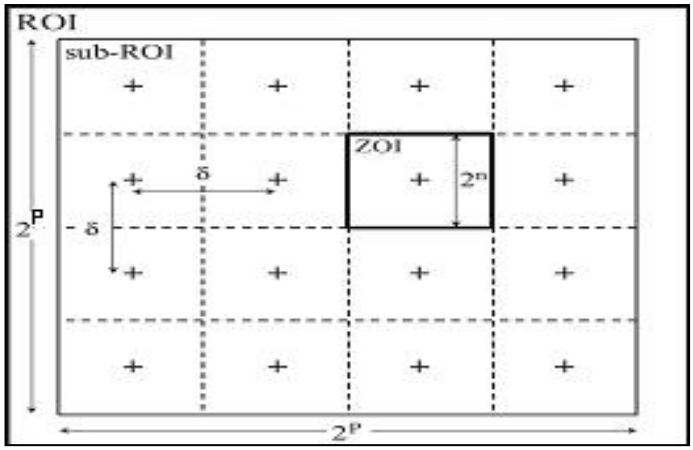

Fig.2. Schematic of the reference image with the Parameters (Q=P and shift δ)

The aim of the paper is to analyze the wrist extension, a remedy for CTS, through a non contact optical technique of Digital Image Correlation (DIC). The aim of the study is to examine the strain pattern on the superficial muscles of the forearm as result of wrist extension. Wrist extension results in relaxation of the wrist. When the wrist is moved into extension position from flexed position, the carpal tunnel expands resulting into the expansion of the tendons which further leads to the relaxation of the median nerve. The effects of stretching on the superficial components of the arm muscles, namely the flexor pollicis longus tendons, abductor pollicis longus tendons and flexor digitorum superficial tendons in the arm and wrist are studied. This can be of significance in further clinical studies.

2. PROBLEM FORMULATION AND EXPERIMENTATION

The setup consists of a desktop computer, a digital camera and the code used to compute the variations in the wrist/wrist positions. The two dimensional variations are measured using the digital image correlation code written by the authors. The position of the camera and the subject are fixed for both pre and post images. The test was conducted on five healthy and active males with no known records of neural/muscular/skeletal disorders. The average height, age and mass of the participants are 170 cm, 35.5 years and 68.5 kg respectively.

The experiment is started by coating the body part (right forearm anterior portion with zinc powder in order to provide contrast for better identification of marker points. Later, the zinc coated portion is covered with a random black speckle pattern with a marker. The subject is made to sit on a chair and place the forearm at the edge of a table so that view for the camera is not obstructed. Initially the elbow, wrist and palm are aligned in the same plane. The initial relaxed forearm is as shown in Fig.1(a). A CCD camera is placed to take the picture, referred to as reference image, of the forearm. In the next step, the wrist is extended by moving the hand approximately 90 degree about the wrist; the deformed image is shown in Fig.1(b). The same setup is used to capture the picture, referred to as deformed image, in the extended position. Finally, the images captured are used for strain computation. The effects of stretching on the superficial components of the arm muscles, namely the flexor pollicis longus tendons, abductor pollicis longus tendons and flexor digitorum superficial tendons in the arm and wrist, are studied.

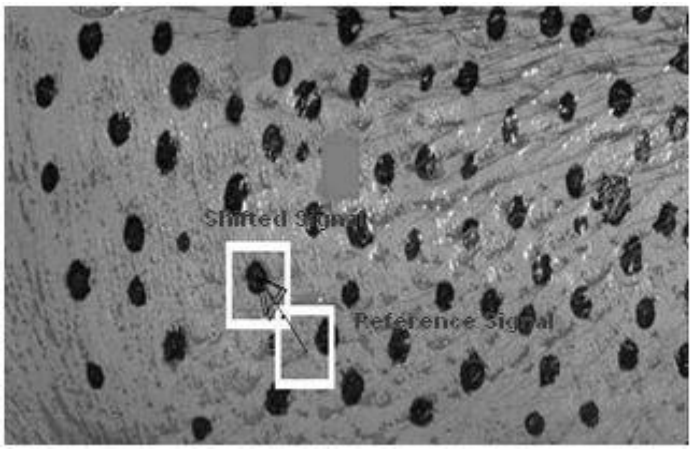

Fig.3. Movement of Zone of Interest from reference position to deformed position

Feature point extraction is the primary step in order to compute the strain pattern. Basic image processing operation of dilation is used in order to extract the feature points from the image. Further, the focus of the algorithm is to match the Zone of Interest of the reference image with the deformed image using a cross correlation function to compute the strain. FFT convolution is used in order to compute the strain for the feature points. The experiment is then repeated for five other subjects and the trends are observed.

3. DISPLACEMENT FIELD MEASUREMENT BY DIGITAL IMAGE CORRELATION

DIC is based on image matching algorithm. It can be effectively used in Fourier as well as physical space. The displacement field of the window under study can be calculated by taking the correlation of the deformed image with respect to the reference image.

3.1 PRELIMINARIES: CORRELATION OF TWO IMAGES

To evaluate the strain field of one image of the deformed surface with respect to reference image, a sub-image is considered which will be referred to as a Zone of Interest (ZOI) Fig.2. The purpose of the correlation method is to match the ZOIs in the respective images.

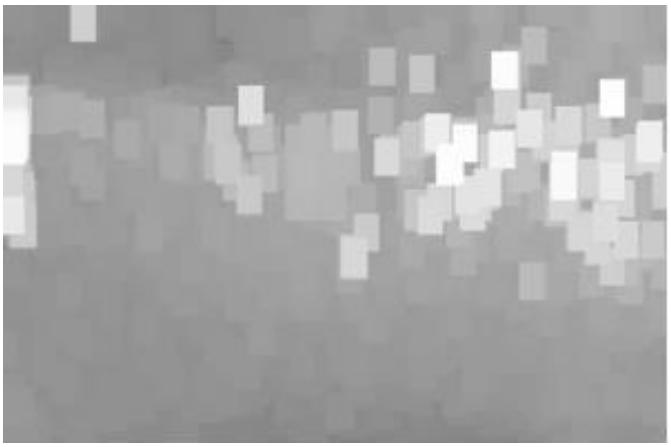

Fig.4(a) Enlargement of area after square 11 by 11 Dilation

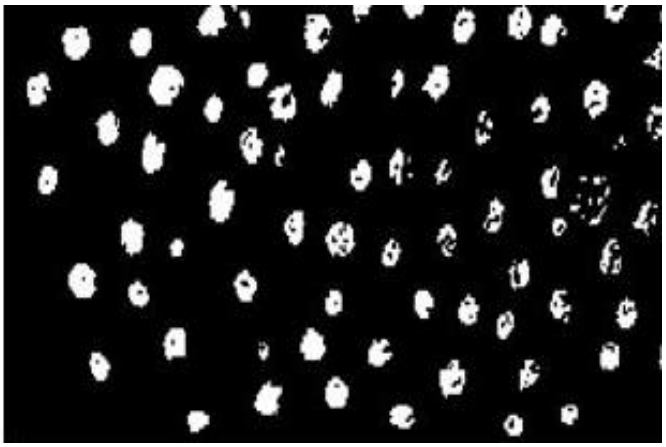

Fig.4(b) Marker points after thresholding

The movement of a ZOI with respect to its copy in deformed image is a two-dimensional shift of an intensity signal digitized by a camera. The aim is to locate the strain signal $g(\xi, \Psi)$, (ZOI in the deformed image) a shifted copy of reference signal $f(\xi, \Psi)$ (ZOI in the reference image) in order to compute the strain as shown in Fig.3. $g(\xi, \Psi)$ can also be considered as equivalent to the reference signal $f(\xi, \Psi)$ shifted by δ_x, δ_y. The strain function can be defined as,

$$g(\xi, \Psi) = f(\xi - \delta_x, \Psi - \delta_y) + b(\xi, \Psi) \quad (1)$$

where, δ_x, δ_y are unknown displacement vectors and $b(\xi, \Psi)$ a random noise. To compute the displacement (δ_x, δ_y) one may minimize the norm of the difference between $f(\xi - x, \Psi - y)$ and $g(\xi, \Psi)$ with respect to x and y,

$$\min_{x,y} \| g(\bullet) - f(\bullet - x, \bullet - y)) \|^2 \quad (2)$$

where '$\bullet$' is a dumpy parameter. If one chooses the usual quadratic norm $\| f \|^2 = \int_{-\infty}^{+\infty}\int_{-\infty}^{+\infty} f(\xi,\psi)\partial\xi\partial\psi$, the previous minimization problem is equal to maximizing the quantity $h(x,y)$:

$$h(x, y) = (g * f)(x, y) = \int_{-\infty-\infty}^{+\infty+\infty} g(\xi, \psi) f(\xi - x, \psi - y)\partial\xi\partial\psi \quad (3)$$

where, '*' denotes the cross-correlation operator. Furthermore, when b is a white noise, the previous estimate is optimal.

$$g * f = FFT^{-1}(FFT[g]\overline{FFT[f]}) \quad (4)$$

The applicability of the 'displacement' property enables one to 'move' a signal. For the sake of simplicity, let us consider the shift operator T_d defined for 1D signals $[T_d f](\xi) = f(\xi - d)$, where d is the shift parameter. The FFT of $T_d f$ becomes $FFT\,[T_d f] = E_d FFT[f]$, where the modulation operator E_d is defined by,

$$[E_d f](\xi) = \exp(-2\pi j \partial\xi) f(\xi) \quad (5)$$

These two results are the basic tools used for image correlation [29].

3.2 CORRELATION ALGORITHM FOR TWO DIMENSIONAL SIGNALS: *CORRELI^{2D}*

In CORRELI [29] algorithm, two images, referred to as 'reference image' and 'deformed image' as shown in Fig.1(a) and Fig.1(b) respectively are considered for strain computation. A region of interest (ROI) centered in the reference image of size $2^p x 2^p$ pixels is selected as shown in Fig.2. The ROI is composed of a number of random elementary regions called ZOIs. The ROI of the same size as in the reference image is selected in the deformed image. A first FFT correlation between the two ROIs results into the average shift U_0, V_0 of the deformed image with respect to the reference image. The maximum of the cross correlation function evaluated for each pixel of the respective ROI is expressed as integer number of pixels representing the shift between the two ROIs. The correlation predicts the maximum number of common pixels between the ROIs. The ROI in the deformed image is positioned at a central point corresponding to the displaced center of the ROI in the reference image by an amount U_0, V_0. In the next step, in order to track the shift for the ZOIs in the reference image, elementary square ZOIs of size $2^s x 2^s$ pixels where s< p are selected in the reference image as shown in Fig. 2. In order to map the whole image, the shift $\delta_x (=\delta_y)$ should be chosen careful such that the shift between two consecutive ZOIs is $1 \le \delta_x \le 2^s$ pixels. The mesh formed by the centers of each ZOI is defined by the two parameters mentioned above, used to analyze the displacement field. Further, the following analysis is performed for each ZOI independently in order to compute the strain for all the ZOIs.

A first FFT correlation of the reference ZOI is carried out with the ROI of the deformed image in order to spot the corresponding ZOI. The correlation results into in plane integral displacement of ΔU, ΔV for the reference ZOI. The displacement correction for the ZOI is completed by displacing the reference ZOI by an additional amount ΔU, ΔV. To limit the errors due to edge effects the considered ZOI is then windowed by a modified Hanning window,

$$\overline{ZOI} = ZOI(H \otimes H) \quad (7)$$

where, $\overline{ZOI}$ denotes the windowed ZOI, $\otimes$ the dyadic product and H the one dimensional modified Hanning window,

$$H(i)=\begin{cases}\frac{1}{2}\left[1-\cos\left(\frac{4\pi i}{2^s-1}\right)\right] & when \quad 0 \le i \le 2^{s-2} \\ 1 & when \quad 2^{s-2} \le i \le 3\times 2^{s-2} \\ \frac{1}{2}\left[1-\cos\left(\frac{4\pi i}{2^s-1}\right)\right] & when \quad 3\times 2^{s-2} \le i \le 2^s-1\end{cases} \quad (8)$$

The value 2^{s-2} is considered as an optimal value to minimize the error due to edge effects [56].

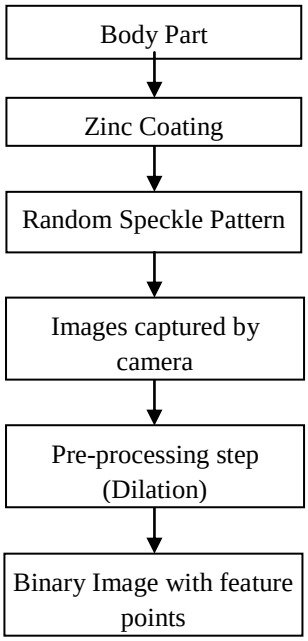

Fig.5. Flow chart for feature extraction

The displacement residues are reduced to lesser than ½ pixels in every direction. A sub-pixel iterative scheme is made to pin point the position of ZOI by computing the remaining displacement. A sub-pixel correlation of the shift δU, δV is calculated by determining the maximum of a parabolic interpolation of the respective correlation function. Shifting-modulation' property of the Fourier Transform is used to move the deformed ZOI by an amount $-\delta U$, $-\delta V$. Some errors can be induced since an interpolation was used. A re-iterating scheme is considering for the new 'deformed' ZOI until a convergence is reached. The criterion checks the increase in the maximum value of the correlation function with the increase in the number of iterations. Otherwise, the iteration scheme is stopped.

4. RESULTS

The strain on the superficial muscles of the forearm resulting due to wrist extension is evaluated by DIC using cross correlation FFT analysis between the referred and the deformed images. FFT computation between two images, an intermediate step of the algorithm is performed using windows of variable sizes. The simulations are evaluated on an Intel Core 2 Duo 2.20 GHz machine. The zone of interest from the reference image shown in Fig.1(a) is convoluted with each region of interest in the deformed image as shown in Fig.1(b), in order to locate the shifted position of the reference zone of interest. A high greyscale peak is obtained on convolution of the reference zone of interest with its shifted copy in the deformed image. Once the zone of interest is located in the deformed image the strain can be computed. The strain fields in both the directions are computed with respect to the reference point marked on the wrist as shown in Fig.1(a). The reference point refers to the point with respect to which all the strain fields are measured. The results are finally analyzed accordingly.

In order to extract the feature points from the image, dilation in a specified 11 by 11 square neighborhood is applied for the enlargement or expansion of region of interest as shown in Fig.4(a). In the next step, a threshold of gray scale 50 is applied to extract all the feature points below the respective value. The feature point's colored black can be extracted easily as they have a grayscale of zero and appear as white or binary 1 on inversion while the background turns black as shown in Fig.4(b). The process is explained in detail in the flow chart shown in Fig.5.

The feature points are extracted using the Matlab pseudo code shown in Fig.6(a). Once the feature points have been extracted the strain can be computed by using FFT convolution between the reference and deformed images. The Matlab pseudo code for the FFT cross correlation is shown in Fig.6(b).

In order to compute the shift between two images, a square ROI of size 512 x 512 pixels is considered in the reference image, to cover maximum number of pixels. A variable zone of interest is considered by computing the height and width of the patch. A total of 64 ZOI are considered for correlation between both the images. On convolution between the images, a high grayscale is observed when the reference zone of interest in the reference image is convoluted with the same zone of interest in the deformed image as shown in Fig.6(c). The reference ZOI is correlated with every ZOI of the deformed image. A high gray scale value of 247 is observed on correlation of reference ZOI with its shifted copy in the deformed image. The minute displacement of 64 pixels in each direction is evaluated by calculating the maximum of a parabolic interpolation of the correlation function after reducing the errors due to edge effects. The process is re-iterated in order to avoid the errors due to parabolic interpolation. The pseudo code can be used to calculate the shift between two consecutive images. *D*2 and *D*1 represents the reference and deformed grayscale images respectively, while *g*2 is the resulting correlation, between the two images as shown in Fig.6(b).

Pseudo Code

```
I=imread ();
I=imresize (I, .25);
D=rgb2gray (l);
Se1 = strel ('square'.11);
K=imdilate (D, se1);
P=D (:,:)<50;
D1 =Image1;
D2=Image2;
g2=ifft2 ((fft2 ((D1)))).*fft2 ((D2)));
```

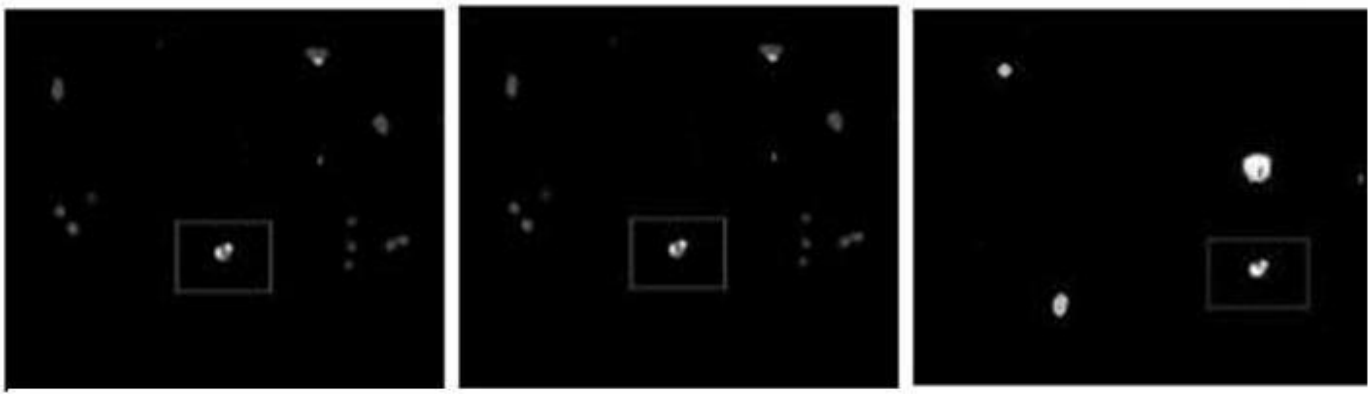

Fig.6(a). Code for extracting the feature points and for computing cross correlation between the two images (b). Intermediate Cross Convolution FFT Step for DIC algorithm (c). High greyscale peak observed on convolution between two ZOIs

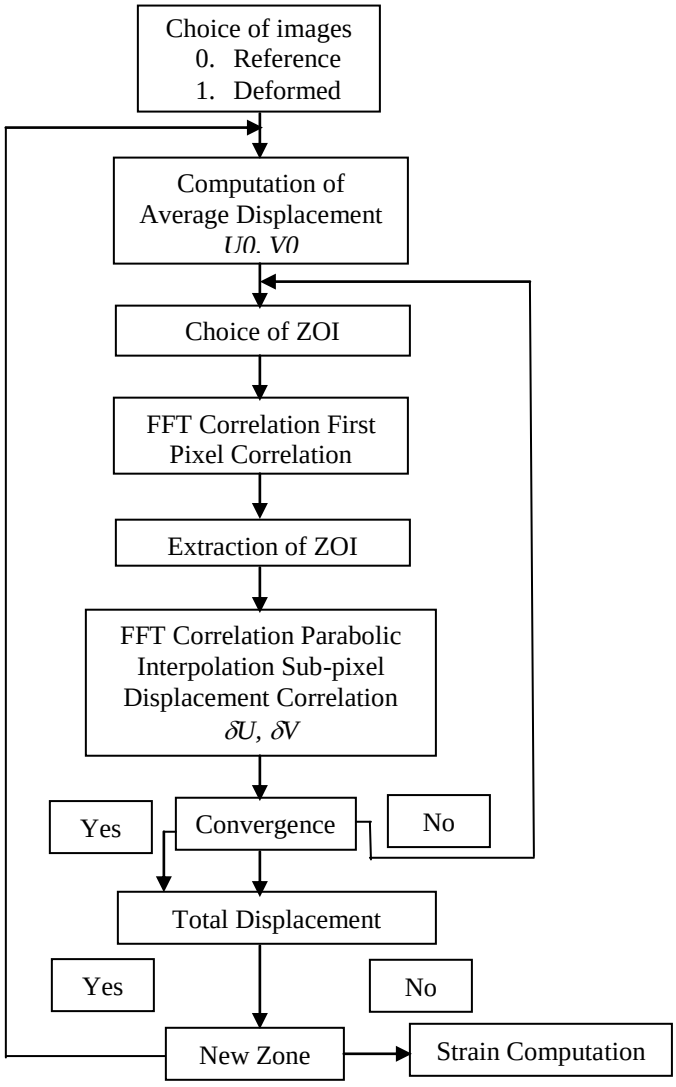

Fig.7. Flow chart for strain computation

Strain field can be easily computed once the shifted ZOI has been located in the deformed image. The strain is computed using the strategy described in Fig.7. The strain along X-plane is computed along X-axis as shown in Fig.1(a). The strain is evaluated along a line a-b formulated in a way such that one end of the line is near the reference point while the other is near the wrist as shown in Fig.8(a). The point 'a' corresponds to the point near to the wrist while point 'b' is the farther end on the line a-b. When the wrist is extended the flexor pollicis longus tendons, abductor pollicis longus tendons and flexor digitorum superficial tendons are extended. The strain field is observed to be maximum at point 'a' as the flexor tendons experience the

utmost stretch in close proximity to the wrist while minimum at the farthest end of the line at point 'b' as the stretch in the tendons goes on decreasing while moving towards the elbow away from the wrist. The statement is supported by the X- plain strain field plot as shown in Fig.8(a). The highest strain of 1.43 mm is experienced by point 'a' while the strain is minimum at point 'b' with a value of 0.27 mm.

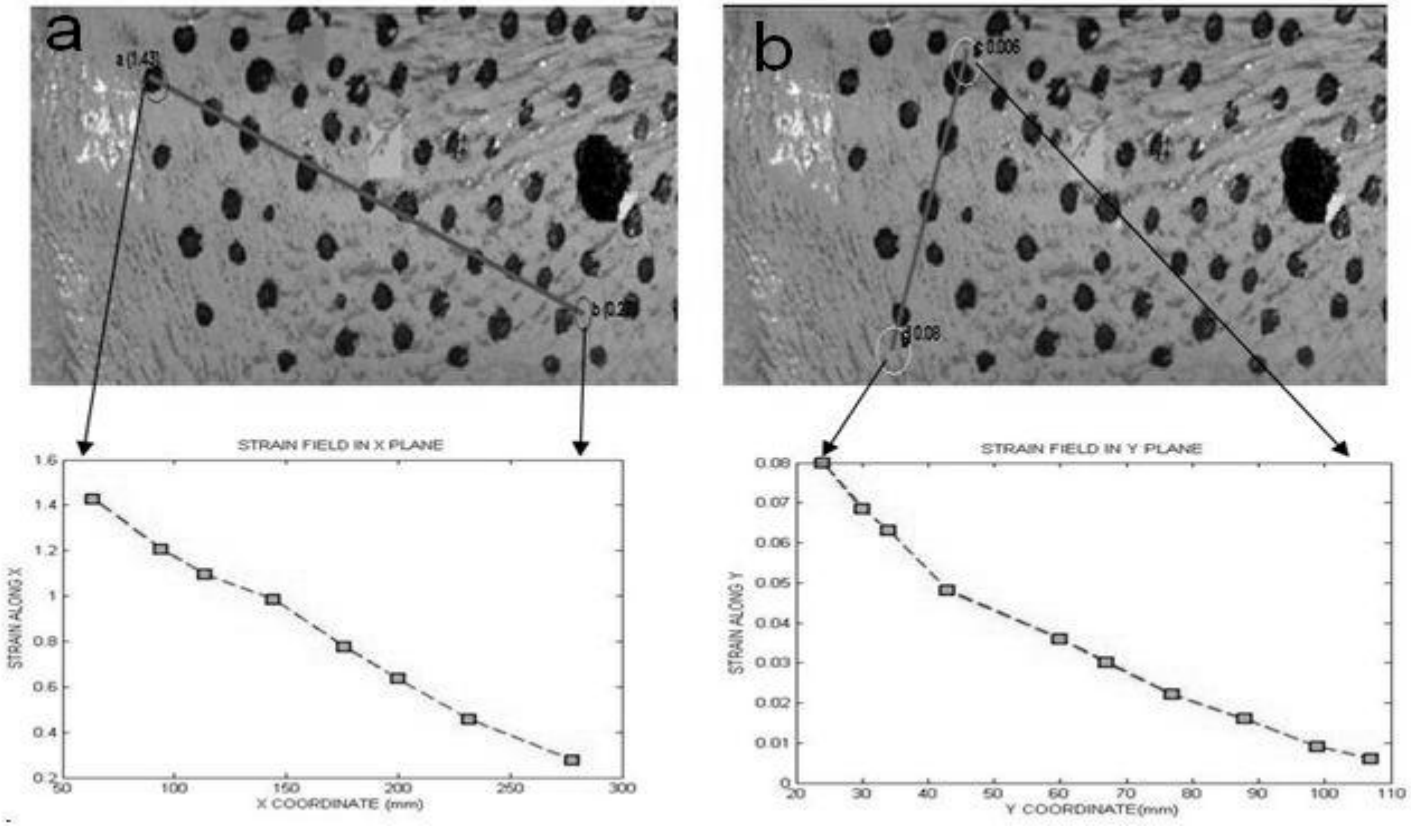

Fig.8(a). Strain Field in the X plane with a minimum with a minimum value of 0.27 mm and a maximum of 1.43 mm (b). Strain Field in the Y plane value of 0.006 mm and a maximum of 0.08 mm

The strain field along Y-plane is computed along Y-axis as shown in Fig.1(a). The strain is evaluated along a line c-d formulated in a way such that one end of the line is near the wrist in the area having high strain. The point 'c' represents the point near to the wrist while the point'd' corresponds to the distant end on the line c-d. The strain field in the Y plane is extremely small as compared to the strain field experienced by the tendons in the X- plane. Point 'c' is relatively near to the wrist as compared to point'd' as a result of which the strain is supplementary at point 'c' as compared to the farthest end point 'd' along the line c-d. The stretch in the tendons goes on decreasing as we move towards the wrist in the similar way compared to X-plane. The above statements are supported by the Y-plane strain field plot as shown in Fig.8(b). The highest strain of 0.06 mm is experienced at point 'c' while the minimum strain at point'd' with a value of 0.008 mm.

5. CONCLUSION

The paper presents a generic methodology to compute the strain pattern for wrist extension experiment, a cure for carpal tunnel syndrome. It is very important and essential to understand the contraction and elongation behavior of the superficial flexor tendons with respect to the force applied on the wrist as the primary knowledge gained will assists us to generate muscle-tendon units which can resulting into better understanding of the force and energy production. The simulations can be further used to get applicable information regarding input parameters for simulation models of the human system as well as to examine aponeuroses to physical activity. This system will also help physiotherapists, surgeons and practitioners to educate themselves and refine their work related to CTS. The study will finally play a vital role in avoiding CTS.

REFERENCES

[1] Mable ET., *"The Thinking Body"*, 1st Ed. Princeton Book Company Publishers, 1988.

[2] Armstrong, Thomas J., Radwin, Robert G., Hansen, Doan J.; Kennedy AND Kenneth W, "Repetitive Trauma Disorders: Job Evaluation and Design, Human Factors", *The Journal of the Human Factors and Ergonomics Society*, Vol. 28, No. 3, pp. 325-336, 1986.

[3] Teixeira, Tania, "*The mouse is biting some PC users*", BBC News, 9th December 2008.

[4] Nahit ES, Pritchard CM, Cherry NM, Silman AJ and Macfarlane GJ, "The influence of work related psychosocial factors and psychological distress on regional musculoskeletal pain: a study of newly employed workers",

*Journal of Rheumatol*ogy, Vol. 28, No.6, pp. 1378–84, 2001.

[5] P. Michael Leahy, "Improved Treatments for Carpal Tunnel and Related Syndromes", http://www.activereleasetechnique.com/pdf/Treatments-Carpal-Tunnel.pdf

[6] Carpal Tunnel Syndrome, Department of Health and Human services, USA. http://www.womenshealth.gov/faq/carpal-tunnel-syndrome.pdf

[7] Kao SY, "Carpal tunnel syndrome as an occupational disease", *The Journal of the American Board of Family Practice / American Board of Family Practice*, Vol. 16, No.6, pp 533–42, 2003.

[8] Lozano-Calderón, Santiago; Shawn Anthony and David Ring, "The Quality and Strength of Evidence for Etiology: Example of Carpal Tunnel Syndrome", *Journal of Hand Surgery*, Vol. 33, No.4, pp 525–538, 2008.

[9] Gross, Brian, Dean Louis, Kyle Carr, and Sharon Weiss, "Carpal Tunnel Syndrome: A Clinicopathollogic Study", *Journal of Environmental Medicine*, pp 437-441, 1995.

[10] Derebery J, "Work-related carpal tunnel syndrome: the facts and the myths", *Clinics in Occupational and Environmental Medicine*, Vol. 5, No.2, pp. 353–67, 2006.

[11] M. o'donnell, A. R. Skovoroda, B. M. Shapo, and S. Y. Emelianov, "Internal displacement and strain imaging using ultrasonic speckle tracking," *IEEE Transaction on Ultrasonics, Ferroelectrics and Frequency Control*, Vol. 41, No. 3, pp. 314–325, 1994.

[12] P. Chaturvedi, M. Insana, and T. Hall, "2-d companding for noise reduction in strain imaging," *IEEE Transaction on Ultrasonics, Ferroelectrics and Frequency Control*, Vol. 45, No. 1, pp. 179–191, 1998.

[13] X. C. Chen, M. J. Zohdy, S. Y. Emelianov, and M. O'donnell, "lateral speckle tracking using synthetic lateral phase," *IEEE Transaction on Ultrasonics, Ferroelectrics and Frequency Control*, Vol. 51, No. 5, pp. 540–550, 2004.

[14] J. D'hooge, A. Heimdal, F. Jamal, T. Kukulski, B. Bijnens, F. Rademakers, l. Hatle, P. Suetens, and G. R. sutherland, "Regional strain and strain rate measurements by cardiac ultrasound: principles, implementation and limitations," *European Journal of Echocardiography*, Vol. 1, No. 3, pp. 154–170, 2000.

[15] B. S Garra, E. I. Cespedes, J. Ophir, S. R. Spratt, R. A. Zuurbier, C. M. Magnant, and M. F. Pennanen, "Elastography of breast lesions: Initial clinical results," *Radiology*, Vol. 202, No. 1, pp. 79–86, 1997.

[16] E. E. Konofagou, T. Varghese, and J. Ophir, "Theoretical bounds on the estimation of transverse displacement, transverse strain and poisson's ratio in elastography," *Ultrasonic. Imaging*, Vol. 22, No. 3, pp. 153–177, 2000.

[17] A. Thitaikumar, T. A. Krouskop, B. S. Garra, and J. Ophir, "Visualization of bonding at an inclusion boundary using axial-shear strain elastography: a feasibility study," *Physics in Medicine and Biology*, Vol. 52, No. 9, pp. 2615–2633, 2007.

[18] A. R. Ahlgren, M. Cinthio, S. Steen, H. W. Persson, T. Sjoberg, and K. Lindstrom, "Effects of adrenaline on longitudinal arterial lopata et al.: estimation of strain in shearing and rotating structures 863 wall movements and resulting intramural shear strain: a first report", *Clinical Physiology and Functional Imaging*, Vol. 29, No. 5, pp. 353–359, 2009.

[19] W. Han, M. X. Xie, X. F. Wang, Q. Lu, J. Wang, L. Zhang, and J. Zhang, "Assessment of left ventricular torsion in patients with anterior wall myocardial infarction before and after revascularization using speckle tracking imaging," *Chinese Medical Journal(Engl.)*, Vol. 121, No. 16, pp. 1543–1548, 2008.

[20] S W Kirkpatrick, M Schroeder and J W Simons, "Evaluation of Passenger Rail Vehicle Crashworthiness", *International Journal of Crashworthiness*, Vol. 6, No. 1, pp. 95-106, 2001.

[21] Marzougui, D., Eskandarian, A. and Mechzkowski, L., " Analysis and Evaluation of a Redesigned 3" x 3" Slipbase Sign Support System Using Finite Element Simulations", *International Journal of Crashworthiness, Woodhead Publishing Ltd, Cambridge*, Vol. 4, No. 1, 1999.

[22] Watanabe, K., Koseki, J. and Tateyama, M., "Application of High-Speed Digital CCD Cameras to Observe Static and Dynamic Deformation Characteristics of Sand", *Geotechnical Testing Journal*, Vol. 28, No. 5, 2005.

[23] Thurner, P., Erickson, B., and Schriock, Z, et. al., "High-Speed Photography of Human Trabecular Bone during Compression", *Proceedings of the Materials Research Society Symposium*, Vol. 874, 2005.

[24] C. A. Walker, "Moiré interferometry for strain analysis", in *Optics and Lasers in Engineering*, Vol. 8, No. 3-4, pp 213-262, 1988.

[25] T. Puškar, , D. Jevremović, L. Blažić, , D. Vasiljević, , D. Pantelić, B. Murić, and B. Trifković, "Holographic interferometry as a method for measuring strain caused by polymerization shrinkage of dental composite", *Contemporary Materials*, Vol. 1, No.1, pp 105-111, 2010.

[26] A R Luxmoore, F A A Amin, and W T Evans, "In-plane strain measurement by speckle photography: A practical assessment of the use of Young's fringes", *The Journal of Strain Analysis for Engineering Design*, Vol. 9, No.1, pp 26-35, 1974.

[27] Lichtenberger R and Schreier H, "Contactless and full-field 3d-deformation measurement for impact and crash tests", *Proceedings of 7th International Symposium and Exhibition on Sophisticated CAR Occupant Safety Systems – AIRBAG*, pp. 40.1 – 40.8, 2004.

[28] Peters W. H and Ransom W. F, "Digital Imaging techniques in experimental analysis", *Optical Engineering*, Vol. 21, pp 427 – 431, 1982

[29] Herd, F. Perie, J.N., and Coret, M., "Mesure de champs de de-placements 2D par Interpolation D'images: CORRELI", *Internal repot (LMT-cachan), internal report 230*, 1999.

[30] Sutton M.A, Cheng M, Peters W.H., Chao Y.J and McNeill S.R, "Application of an optimized digital correlation

method to planar deformation analysis", *Image and Vision Computing*, Vol. 4, pp 143-151, 1986.

[31] Kevin M. Moerman, Cathy A. Holt, Sam L. Evans, and Ciaran K. Simms, "Digital image correlation and finite element modelling as a method to determine mechanical properties of human soft tissue in vivo", *Journal of Biomechanics*, Vol. 42, No. 8, 29 pp 1150-1153, 2009.

[32] Wang C.C.B, Deng J.M, Ateshian G.A and Hung C.T, "An automated approach for direct measurement of two-dimensional strain distributions within articular cartilage under unconfined compression", *Journal of Biomechanical Engineering*, Vol. 124, pp 557–67, 2002.

[33] Nicolella D. P, Moravits D. E, Gale A. M, Bonewald L. F and Lankford J, "Osteocyte lacunae tissue strain in cortical bone", *Journal of Biomechanics*, Vol. 39, pp 1735–1743, 2006.

[34] Thompson M S, Schell H, Lienau J and Duda G N, "Digital image correlation: A technique for determining local mechanical conditions within early bone callus", *Medical Engineering & Physics*, Vol. 2, pp 820–823, 2007.

[35] Zhou, P. and Goodson, K. E., "Sub-pixel Displacement and Deformation Gradient Measurement Using Digital Image-Speckle Correlation (DISC)", *Optical Engineering*, Vol. 40, No. 8, pp 1613-1620, 2001.

[36] Yogel, D., Grosser, V., Schubert, A. and Michel, B., "MicroDAC Strain Measurement for Electronics Packaging Structures", *Optics and Lasers in Engineering*, Vol. 36, pp. 195-211, 2001.

[37] Srinivasan, V., Radhakrishnan, S., Zhang, X., Subbarayan, G., Baughn, T. and Nguyen, L., "High Resolution Characterization of Materials Used In Packages through Digital Image Correlation", *ASME/Pacific Rim Technical Conference and Exhibition on Integration and Packaging of MEMS, NEMS and Electronic Systems*, pp. 17-22, 2005.

[38] Sutton, M.A., Cheng, M., Peters, W.H., Chao, Y.J and McNeill, S.R, "Application of an optimized digital correlation method to planar deformation analysis", *Image and Vision Computing*, Vol. 4, No.3, pp. 143-151, 1986

[39] Reu, P. and Miller, T., "High-speed Multi-camera DIC for Finite Element Model Validation", *Part 1, SEM Annual Conference and Exposition on Experimental and Applied Mechanics*, 2006.

[40] Tiwari, V., Williams, S., Sutton, M. and McNeill, S., "Application of Digital Image Correlation in Impact Testing", *Proceedings of the 2005 SEM Annual Conference and Exposition on Experimental and Applied Mechanics*, 2005.

[41] Kehoe, L., Lynch, P. and Guénebaut, V., "Measurement of Deformation and Strain in First Level C4 Interconnect and Stacked Die using Optical Digital Image Correlation", *Electronic Components and Technology Conference*, pp. 1874-1881, 2006.

[42] Cheng, T., Dai, C. and Gan, R., "Viscoelastic Properties of Human Tympanic Membrane", *Annals of Biomedical Engineering*, Vol. 35, No. 2, pp 305-314, 2007.

[43] Myers, K. M., Paskaleva, A. P., House, M. and Socrate, S., "Mechanical and biochemical properties of human cervical tissue", *Acta Biomaterialia* , Vol. 4, No. 1, pp 104-116, 2008.

[44] Boyce, B. L., Grazier, J. M., Jones, R. E. and Nguyen, T. D., "Full-field deformation of bovine cornea under constrained inflation conditions", *Biomaterials*, Vol. 29, No. 28, pp 3896-3904, 2008.

[45] Sutton, M. A., Ke, X., Lessner, S. M., Goldbach, M., Yost, M., Zhao, F. and Schreier, H. W., "Strain field measurements on mouse carotid arteries using microscopic three-dimensional digital image correlation" *Journal of Biomedical Materials Research Part A*, Vol. 84A, No. 1, pp 178-190, 2008.

[46] Bonetto P, Comis G, Formiconi AR and Guarracino M.A, "New approach to brain imaging, based on an open and distributed environment", Proceedings *of International IEEE EMBS Conference on Neural Engineering*, 2003.

[47] Chu, T.C., Ranson, W.F., Sutton, M.A. and Petters, W.H, "Applications of Digital-Image-Correlation Techniques to Experimental Mechanics", *Experimental Mechanics*, Vol. 3, No.25, pp 232-244, 1985.

[48] Chiang F.P, Wang Q. and Lehman F., "New developments in full-field strain measurements use speckles", *In: ASTMSTP 1318 on Non-traditional Methods of Sensing Stress, Strain and Damage in Materials and Structures*, pp 156–170, 1997.

[49] Chen J L, Xia G M, Zhou K B, Xia G S and Qin Y W, "Two-step digital image correlation for micro-region measurement", *Optics and Lasers in Engineering*, Vol. 43, No. 8, pp 836–46, 2005.

[50] Zhang Z F, Kang Y L,Wang HW, Qin Q H, Qiu Y and Li X Q, " A novel coarse–fine search scheme for digital image correlation method ", *Measurement- Elsevier*, Vol 39, No. 8, pp: 710–8, 2006.

[51] Wang M, Wang H and Cen Y, "High-speed digital-image correlation method", *Optics Letters*. Vol. 34, No. 13, pp. 1955–1957, 2009.